J|A|C|S ARTICLES

Published on Web 05/11/2009

A New Perovskite Polytype in the High-Pressure Sequence of $BaIrO_3$

Jin-Guang Cheng,[†] José Antonio Alonso,*[,†,‡] Emmanuelle Suard,[§] Jian-Shi Zhou,[†] and John B. Goodenough[†]

Texas Materials Institute, ETC 9.102, The University of Texas at Austin, Austin, Texas, 78712, Instituto de Ciencia de Materiales de Madrid, CSIC, Cantoblanco, E-28049 Madrid, Spain, and Institute Laue-Langevin (ILL) 156X, F-38042 Grenoble Cedex 9, France

Received March 9, 2009; E-mail: ja.alonso@icmm.csic.es

Abstract: The high-pressure sequence of the perovskite polytypes of $BaIrO_3$ has been investigated in the pressure range up to 10 GPa. At ambient pressure the so-called "9R" polytype has been prepared by solid-state reaction and slow cooling in air to yield an almost fully oxygen-stoichiometric $BaIrO_{2.96(1)}$ composition. The crystal structure has been refined from XRD data in the monoclinic *C*2/*m* space group with $a = 10.0046(3)$ Å, $b = 5.75362(14)$ Å, $c = 15.1839(4)$ Å, $\beta = 103.27(1)°$; it contains trimers of face-sharing octahedra (or Ir_3O_{12} trioctahedra) that are linked by their vertices to form columns parallel to the *c*-axis with a stacking of layers of corner sharing (*c*) and face sharing (*h*) IrO_6 octahedra along the sequence *hhchhc*. This structure is stable up to 3 GPa; at 4 GPa a new 5H polytype has been stabilized as a pure phase. The crystal structure has been solved by *ab initio* procedures from powder XRD data. It is monoclinic with $a = 9.9511(2)$ Å, $b = 5.7503(1)$ Å, $c = 13.71003(3)$ Å, $\beta = 118.404(2)°$, and it was refined in the *C*2/*m* space group from NPD data collected at room temperature. This polytype can be described as a stacking of IrO_6 octahedra along the sequence *hchcc*. The structure contains chains of double dimer units of face-sharing octahedra; the twin dimers are connected to single layers of vertex-sharing octahedra, forming infinite chains along *c*. This is a unique stacking that, with this repetition length, has never been described before among the hexagonal polytypes of ABO_3 perovskites. The 5H polytype is stable in a narrow pressure range; at 5 GPa the 6H structure is formed, stable up to 10 GPa. The 6H-$BaIrO_3$ polytype is monoclinic, space group *C*2/*c*, with $a = 5.7483(2)$ Å, $b = 9.9390(3)$ Å, $c = 14.3582(5)$ Å, $\beta = 91.319(2)°$. The structure consists of dimers of face-sharing octahedra separated by single corner-sharing octahedra, showing the sequence *hcchcc* along the *c*-axis. At 10 GPa the cubic 3C perovskite structure could be identified as a minority phase, with $a = 4.0611(7)$ Å, defined in the $Pm\bar{3}m$ space group. The precarious stability of the 5H polytype, as well as the novel pressure sequence displayed by $BaIrO_3$ that is distinct from the classical sequence 9R-4H-6H-3C exhibited by many transition metal oxides, for instance $BaRuO_3$, is a result of the particular stability of the "9R" ambient-pressure structure, which is reinforced by a strong Ir−Ir bond across the octahedral faces, and the Ir−Ir Coulombic repulsion across shared faces that destabilizes the 4H polytype relative to the 6H phase to allow stabilization of the hybrid 5H polytype in a narrow presure range.

Introduction

The magnetic and electronic properties of transition-metal oxides have been extensively studied within the past few years, and materials adopting the ABO_3 perovskite structure have constituted a central theme given the well-recognized flexibility of this structural type to incorporate a wide range of cations at both the 12-coordinate A position and the 6-coordinate B site. The crystal structures can be considered to be built up from the close packing of AO_3 layers with B atoms placed at the all-oxygen octahedral voids. If all of the stacking of AO_3 layers is cubic (*c*) or hexagonal (*h*), the structure will be referred as 3C or 2H, which corresponds to the corner- or face-sharing arrangement of $BO_{6/2}$ octahedra, respectively.

As a rule of thumb, where the tolerance factor [$t \equiv A-O/\sqrt{2}(B-O)$] equals unity, the ideal perovskite structure is stabilized, which can be regarded as a three-dimensional framework built up by vertex-sharing BO_6 octahedra with the large A cation in the 12-coordinated cavities of the framework. Mixed cubic and hexagonal stacking can also be realized, and a wide range of different structural polytypes can be stabilized. The ionic radius, charge, and electronic configuration of the cations, as well as the preparation conditions, can determine the adoption of a particular polytype. The hexagonal-perovskite polytypes are usually formed under ambient pressure in the ABO_3 compounds having a tolerance factor $t > 1$.[1] In between 2H and 3C, polytypes having a different ratio of cubic to hexagonal stacking have been identified, such as 9R (*chhchhchh*), 4H (*chch*), and 6H (*cchcch*). Since high pressure stabilizes preferentially the high density phase, i.e. cubic versus hexagonal stacking, the hexagonal-perovskite polytypes can be transformed gradually in the sequence of 2H-9R-4H-6H-3C

[†] The University of Texas at Austin.
[‡] Instituto de Ciencia de Materiales de Madrid.
[§] Institute Laue-Langevin (ILL).

(1) Goodenough, J. B.; Kafalas, J. A.; Longo, J. M. *High-Pressure Synthesis*, Academic Press, Inc.: New York and London, 1972.

under high pressure. For example, the ambient 9R-$BaRuO_3$ was transformed to the 4H phase at 3 GPa, the 6H phase at 5 GPa, and finally the 3C phase at 18 GPa.[2] In addition, it has been shown that the physical properties of $BaRuO_3$ polytypes exhibit a strong dependence on the stacking sequence of $RuO_{6/2}$ octahedra.

Recently, barium iridate, $BaIrO_3$, has attracted much attention due to the observation of charge-density-wave (CDW) formation and weak ferromagnetism at the same temperature $T_C \approx 180$ K.[3−5] In fact, it is the first known ferromagnet that contains a 5d transition metal cation in a ternary oxide. The nonmetallic nature of $BaIrO_3$ makes the observation of a CDW quite unusual. If prepared at ambient pressure, the crystal structure of $BaIrO_3$ is monoclinic (space group $C2/m$) and consists of vertex-linked Ir_3O_{12} trimers with three face-sharing IrO_6 octahedra forming columns roughly parallel to the c-axis.[6] The monoclinic distortion in $BaIrO_3$ is generated by a twisting and buckling of the Ir_3O_{12} trimers that gives rise to zigzag chains along the c-axis. Except for the monoclinic distortion, $BaIrO_3$ has an identical BaO_3 stacking sequence to the 9R-$BaRuO_3$. Longo et al.[7] have reported that the ambient-pressure phase of $SrIrO_3$ has the monoclinically distorted 6H structure, which transforms to the 3C perovskite structure under high pressure and high temperature. By using the precursor route, Chamberland et al.[8] have prepared various $BaIrO_3$ polytypes, such as 3H, 6H, and 18R. It is noteworthy that this 6H-$BaIrO_3$ phase is different from the 6H-$SrIrO_3$. Powell et al.[9] identified, by neutron diffraction, a significant number of oxygen vacancies in a sample of composition $BaIrO_{2.74}$ prepared by quenching the sample from 950 °C, whereas an almost stoichiometric material, $BaIrO_{2.94}$, was synthesized by slowly cooling the sample; both compounds were structurally characterized as the monoclinically distorted polytype related to 9R-$BaRuO_3$. To date, no attempt has been made to characterize the high-pressure phases of $BaIrO_3$. In this work, we have investigated the structural evolution of $BaIrO_3$ under high pressure up to 10 GPa and 1000 °C and identified a new 5H polytype within a very narrow pressure range $3 < P < 5$ GPa, besides a 6H phase at $P > 5$ GPa and a 3C perovskite at 10 GPa as a minority phase. In $BaIrO_3$, the competition between the Coulombic repulsion of Ir^{4+} ions and the strong Ir−Ir bonding through face-sharing octahedra, with long equilibrium distances due to the 5d nature of the external Ir orbitals, is the origin of the distinct pressure evolution of the different polytypes identified in this study.

Experimental Section

The ambient-pressure phase, which will be labeled hereafter as "9R"-$BaIrO_3$, was synthesized by using a conventional solid-state reaction. Stoichiometric mixtures of $BaCO_3$ and Ir metal were thoroughly mixed in an agate mortar and sintered up to 1000 °C for 4 days with several intermediate grindings. The high-temperature and high-pressure (HTHP) experiments were performed in a Walker-type, multianvil pressure module. Semisintered Ceramacast 584 (5% Cr_2O_3) octahedra were used as pressure medium. Several pellets of the 9R-$BaIrO_3$ wrapped with gold foil were put into a boron nitride sleeve and then inserted into a cylindrical graphite heater, which was put in the center of the octahedron. Pyrophyllite plugs were stuffed at both ends of the heater. During the HTHP experiment, the sample was first compressed to the desired pressure by eight truncated tungsten carbide cubes with TEL = 8 mm. Then, the temperature was increased to 1000 °C and kept for 30 min before quenching to room temperature.

A thermal analysis (TGA curve) in reducing conditions (5% H_2/95% Ar flow) of the ambient-pressure phase was performed in a Perkin-Elmer TGA 7 apparatus in the temperature range between 25 and 730 °C with a heating rate of 1 °C/min. About 50 mg of sample were used in the experiment.

XRD patterns were collected at 295 K with Cu Kα radiation in a Philips X'pert diffractometer by step-scanning from 10 to 120° in 2θ in increments of 0.02° and a counting time of 10 s each step. The neutron powder diffraction (NPD) diagram of 5H-$BaIrO_3$ was collected at 295 K in the high-resolution D2B diffractometer at ILL-Grenoble. A wavelength of 1.594 Å was selected from a Ge monochromator. The counting time was 12 h, with 0.4 g of sample contained in a vanadium can. The sample was obtained by gathering the product of 8 HPHT experiments (50 mg each). The crystal structure of the 5H phase was resolved by direct methods with the EXPO program[10] from XRD data. For the XRD and NPD profile refinements (FULLPROF program[11]) a pseudo-Voigt function was chosen to generate the line shape of the diffraction peaks. The coherent scattering lengths in the NPD refinements for Ba, Ir, and O were 5.070, 10.60, and 5.803 fm. The neutron absorption of Ir was corrected with a μr value of 1.90 estimated for the diameter of the sample cylinder. The location of oxygen atoms was performed by Fourier synthesis with the FOURIER program[12] included in the FULLPROF suite. In the final refinement run, the following parameters were refined: background coefficients, zero-point, half-width, and pseudo-Voigt parameters for the peak shape; scale factor, positional parameters, occupancy factors for oxygen atoms (NPD data only), thermal isotropic factors, and unit cell parameters.

Results

Four different polytypes of $BaIrO_3$ were identified as a function of the synthesis pressure. In the pressure range $0 \le P \le 3$ GPa, the "9R" polytype was found; in a narrow pressure interval around 4 GPa a new polytype, called hereafter 5H, was identified; finally, in the $5 \le P \le 10$ GPa range, the 6H polytype could be stabilized; and at 10 GPa the cubic 3C perovskite could be identified as a minority phase.

"9R" Polytype. The ambient-pressure phase of $BaIrO_{3-\delta}$ was obtained as a black polycrystalline powder. The oxygen content (3-δ) was determined by thermogravimetric analysis in a H_2/Ar flow. The inset of Figure 1 shows the TGA curve. The starting material was decomposed in two successive steps to give a mixture of BaO + Ir metal. The total weight loss of 8.8% corresponds to 1.96(1) oxygen atoms, implying a starting composition of $BaIrO_{2.96(1)}$, close to the full oxygen stoichiometry. The XRD pattern of this ambient-pressure phase (Figure 1) could be indexed in a monoclinic unit cell with a = 10.0046(3) Å, b = 5.75362(14) Å, c = 15.1839(4) Å, β =

(2) Jin, C.-Q.; Zhou, J.-S.; Goodenough, J. B.; Liu, Q. Q.; Zhao, J. G.; Yang, L. X.; Yu, Y.; Yu, R. C.; Katsura, T.; Shatskiy, A.; Ito, E. *Proc. Natl. Acad. Sci. U.S.A.* **2008**, *105*, 7115.
(3) Cao, G.; Crow, J. E.; Guertin, R. P.; Henning, P. F.; Homes, C. C.; Strongin, M.; Basov, D. N.; Lochner, E. *Solid State Commun.* **2000**, *113*, 657.
(4) Whangbo, M.-H.; Koo, H.-J. *Solid State Commun.* **2001**, *118*, 491.
(5) Maiti, K.; Singh, R. S.; Medicheria, V. R. R.; Rayaprol, S.; Sampathkumaran, E. V. *Phys. Rev. Lett.* **2005**, *95*, 016404.
(6) Siegrist, T.; Chamberland, B. L. *J. Less-Common Met.* **1991**, *170*, 93.
(7) Longo, J. M.; Kafalas, J. A.; Arnott, R. J. *J. Solid State Chem.* **1971**, *3*, 174.
(8) Chamberland, B. L. *J. Less-Common Met.* **1991**, *171*, 377.
(9) Powell, A. V.; Battle, P. D. *J. Alloys Compd.* **1996**, *232*, 147.
(10) Altomare, A.; Burla, M. C.; Cascarano, G.; Giacovazzo, C.; Guagliardi, A.; Moliterni, A. G. G.; Polidori, G. G. *J. Appl. Crystallogr.* **1995**, *28*, 842. Altomare, A.; Cascarano, G.; Giacovazzo, C.; Guagliardi, A.; Burla, M. C.; Polidori, G.; Camalli, M. *J. Appl. Crystallogr.* **1994**, *27*, 435.
(11) Rodríguez-Carvajal, J. *Physica (Amsterdam)* **1993**, *192B*, 55.
(12) Roisnel, T.; Rodríguez-Carvajal, J. *Mater. Sci. Forum* **2001**, *378−3*, 118.

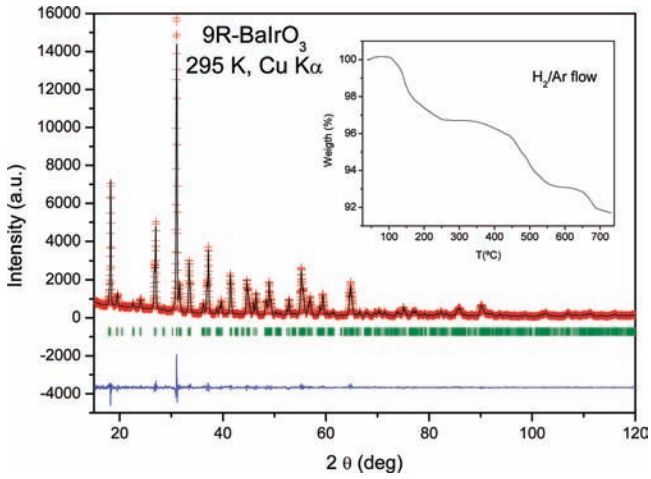

Figure 1. XRD diagram for ambient pressure "9R" $BaIrO_3$, fitted to the model described in the text in the *C*2/*m* space group. Observed profile (crosses), calculated (full line) and difference (down) profiles, with the allowed Bragg reflections as vertical marks. The inset shows the thermogravimetric curve for the ambient-pressure phase, recorded in a H_2/Ar flow.

Table 1. Atomic Coordinates and Isotropic Thermal Factors B_{iso} [Å^2] for "9R"-$BaIrO_3$ from Powder XRD Data[a] at 295 K; Space Group *C*2/*m*, $a = 10.0046(3)$ Å, $b = 5.75362(14)$ Å, $c = 15.1839(4)$ Å, $\beta = 103.27(1)°$, $V = 850.69(4)$ Å^3, $Z = 12$

atom	site	*x*	*y*	*z*	B_{iso}(Å^2)
Ba1	4i	0.7757(5)	0.0	0.2491(4)	1.33
Ba2	4i	0.3689(5)	0.0	0.0733(3)	1.39
Ba3	4i	0.1521(4)	0.0	0.4239(3)	1.52
Ir1	4i	0.0863(3)	0.0	0.17660(18)	0.87
Ir2	2a	0.00000	0.0	0.0	1.19
Ir3	4i	0.4658(3)	0.0	0.32206(18)	0.60
Ir4	2d	0.5	0.0	0.5	0.64
O1	4i	0.301(3)	0.0	0.229(2)	1.4(2)
O2	8i	0.051(2)	0.264(4)	0.2608(17)	1.4(2)
O3	4i	0.879(4)	0.0	0.099(2)	1.4(2)
O4	8j	0.123(2)	0.272(5)	0.0790(17)	1.4(2)
O5	8j	0.386(2)	0.240(5)	0.4038(16)	1.4(2)
O6	4i	0.662(4)	0.0	0.424(2)	1.4(2)

[a] Discrepancy factors: $R_p = 5.32\%$, $R_{wp} = 6.71\%$, $R_{exp} = 5.01\%$, $\chi^2 = 1.79$, $R_{Bragg} = 2.85\%$.

103.27(1)°. These parameters are in excellent agreement with those reported by Siegrist et al.[6] for $BaIrO_3$, of $a = 10.0052(4)$ Å, $b = 5.7514(2)$ Å, $c = 15.1742(7)$ Å, $\beta = 103.274(5)°$, or by Powell et al.[9] for $BaIrO_{2.94}$ of $a = 9.9992(3)$ Å, $b = 5.7490(1)$ Å, $c = 15.1707(2)$ Å, $\beta = 103.27(1)°$. The crystal structure was refined from the powder XRD data in a monoclinically distorted variant of the nine-layer $BaRuO_3$ oxide, in a structural model[6,9] defined in the *C*2/*m* space group, with three kinds of Ba atoms at 4i (*x*,0,*z*) positions, four types of unequivalent Ir atoms at 4i, 2a (0,0,0), and 2d (0.5,0,0.5) sites, and six types of oxygen atoms at 4i and 8j (*x*,*y*,*z*) positions. The final atomic parameters after the Rietveld refinement are listed in Table 1, and the main interatomic distances and angles are gathered in Table 2. Owing to the lack of sensitivity of X-rays to oxygen in the presence of the strong scatterers barium and iridium, no conclusions could be drawn concerning the presence or distribution of oxygen vacancies, which have been described in the "9R" polymorphs of $BaIrO_{2.94}$ and $BaIrO_{2.74}$ by neutron diffraction.[9] Nevertheless, the preparation conditions of the present sample, by slow cooling in air of the specimen as well as the thermal analysis of the oxygen contents, seem to warrant a virtually stoichiometric oxygen content.

Table 2. Main Interatomic Distances (Å) and Angles (deg) of "9R"-$BaIrO_3$ from Powder XRD Data at 295 K

IrO_6octahedral			BaO_{12}cuboctahedra		
Ir1	−O1	2.11(3)	Ba1	−O1	2.910(5) × 2
	−O2	2.07(2) × 2		−O2	3.11(2) × 2
	−O3	2.14(4)		−O2	2.67(2) × 2
	−O4	2.24(3) × 2		−O3	2.71(4)
<Ir1−O>		2.15		−O4	2.99(2) × 2
				−O5	2.79(2) × 2
Ir2	−O3	2.14(4) × 2		−O6	3.12(5)
	−O4	2.17(2) × 4	<Ba1−O>		2.90
<Ir2−O>		2.16			
			Ba2	−O1	2.61(3)
Ir3	−O1	1.91(3)		−O2	3.30(2) × 2
	−O2	1.95(2) × 2		−O3	3.16(3)
	−O5	2.13(3) × 2		−O3	2.902(4) × 2
	−O6	2.20(4)		−O4	2.93(2) × 2
<Ir3−O>	2.05			−O4	2.84(2) × 2
				−O4	2.68(3) × 2
Ir4	−O5	2.14(2) × 4	<Ba2−O>		2.92
	−O6	2.19(5) × 2			
<Ir4−O>	2.17		Ba3	−O2	2.88(2) × 2
<Ir−O>	2.12			−O5	2.79(2) × 2
				−O5	3.01(2) × 2
Ir1	−Ir2	2.622(3)		−O5	3.11(3) × 2
Ir3	−Ir4	2.644(3)		−O6	2.61(4) × 2
				−O6	2.8785(14) × 2
			<Ba3−O>		2.90
Ir1−O1−Ir3		155.4(11)	<Ba−O>		2.91
Ir1−O2−Ir3		164.2(10)			
Ir1−O3−Ir2		75.7(14)			
Ir1−O4−Ir2		72.8(10)			
Ir3−O5−Ir4		76.5(10)			
Ir3−O6−Ir4		73.9(16)			

The goodness of the fit to the XRD data is illustrated in Figure 1, and a view of the crystal structure of the ambient-pressure polytype is shown in Figure 2. It can be described as a stacking of layers of corner sharing (*c*) and face sharing (*h*) IrO_6 octahedra along the sequence *hhchhc*. As an alternative descrip-

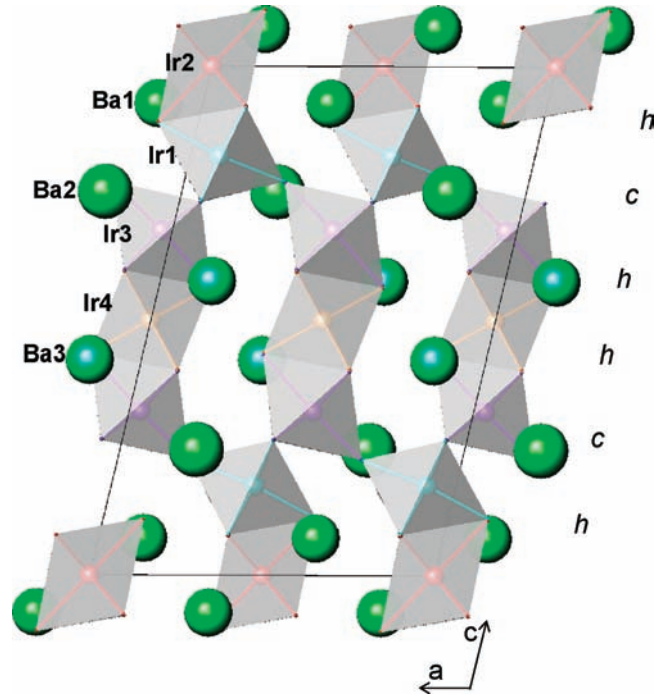

Figure 2. Projection of the "9R" $BaIrO_3$ crystal structure along the [1 0 0] direction, showing the chains of IrO_6 octahedra sharing faces or corners along the *c*-axis according to the stacking sequence *hhchhc*.

tion, trimers of face-sharing octahedra (or Ir_3O_{12} trioctahedra) are linked by their vertices to form columns parallel to the *c*-axis. The monoclinic distortion in $BaIrO_3$ results from a shifting and tilting of the columns relative to each other. Ir1−Ir2 and Ir3−Ir4 distances of 2.622(3) and 2.644(3) Å, are very similar to those described for $BaIrO_{2.94}$,[9] of 2.618(4) and 2.627(4) Å, respectively, which supports a full oxygen stoichiometry for the present compound since these metal−metal distances are very sensitive to the oxygen content of the sample: for oxygen-deficient $BaIrO_{2.74}$, Ir1−Ir2 and Ir3−Ir4 distances were reported to take the values 2.557(7) and 2.619(7) Å, respectively. The observed Ir−Ir distances are even smaller than the separation of 2.72 Å found in Ir metal, which indicates significant interactions between iridium cations at the center of face shared pairs of octahedra.

It was of interest to estimate the valence of the Ir cations by means of the Brown's bond valence model,[13,14] which gives a phenomenological relationship between the formal valence of a bond and the corresponding bond length. The valence is the sum of the individual bond valences (s_i) for Ir−O bonds; the individual bond valences are calculated as $s_i = \exp[(r_0 - r_i)/B]$; $B = 0.37$, $r_0 = 1.870$ for the $Ir^{4+}-O^{2-}$ pair. The bond valences of the four kinds of Ir cations were 2.91+, 2.74+, 3.91+, and 2.76+ for Ir1 to Ir4 atoms, respectively. They are significantly smaller than the expected value of 4+. This is a consequence of the metal−metal bonding within the trimers, where a large fraction of the bonding power of Ir is used. In fact, the lowest valence is observed for Ir2 and Ir4, which are located in the center of the trimers (Figure 2) and therefore are expected to present a higher contribution of metal−metal bonding.

The oxygen-coordination polyhedra of the Ba atoms are very irregular, with Ba−O distances ranging from 2.61(3) Å for Ba2−O1 to 3.30(2) Å for Ba2−O2. For Ba1 and Ba2, the bond-length distribution is formed by 5 short + 7 long Ba−O distances, whereas for Ba3 there are 3 short + 8 long distances, with the 12th bonding longer than 3.5 Å. The average <Ba−O> bond lengths are very similar for the three Ba atoms, between 2.90 and 2.92 Å.

It is important to notice that, although this polytype has been compared to the 9R ambient pressure phase of $BaRuO_3$, with rhombohedral symmetry, unit cell parameters $a = 5.755$, $c = 21.621$ Å[15] and a stacking sequence $(hhc)_3$, the monoclinic distortion described for ambient-pressure $BaIrO_3$ involves a shorter periodicity, with a stacking sequence $(hhc)_2$ along the *c*-axis, as is shown in Figure 2. It is worth mentioning that Mn-doped $BaIrO_3$, prepared at ambient pressure, exhibits the 9R structure, defined in the space group $R\bar{3}m$ with $a \approx 5.7$ Å and $c \approx 21.4$ Å, in the compositional range $BaIr_xMn_{1-x}O_3$, $x = 0.3$, 0.4, and 0.5.[16]

5H Polytype. The XRD pattern of 5H-$BaIrO_3$ (Figure 3) obtained at 4 GPa could be indexed in a monoclinic unit cell with the JADE program to give the parameters $a = 9.9511(2)$ Å, $b = 5.7503(1)$ Å, $c = 13.71003(3)$ Å, $\beta = 118.404(2)°$. The systematic absences were consistent with the *C*2/*m* space group. The estimated crystallographic density from that of the "9R" polytype yielded $Z = 10$. The crystal structure was solved by direct methods from powder XRD data with the EXPO program,[10] which enabled the localization of the Ba and Ir atoms. The oxygen atoms were located in successive Fourier synthesis. The exact position of the oxygen atoms was refined from NPD data.

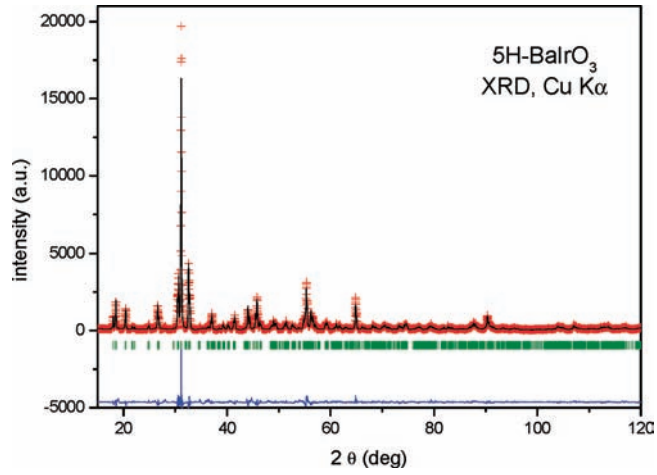

Figure 3. XRD pattern of the 5H−$BaIrO_3$ polytype, obtained at 4 GPa. The figure shows the Rietveld plot after the structural refinement of the model described in the text, in the monoclinic space group *C*2/*m*.

Table 3. Atomic Coordinates and Isotropic Thermal Factors B_{iso} for 5H-$BaIrO_3$ from NPD Data[a] at 295 K; Space Group *C*2/*m*, $a = 9.9554(8)$ Å, $b = 5.7434(6)$ Å, $c = 13.8049(12)$ Å, $\beta = 119.231(6)°$, $V = 688.8(1)$ Å^3, $Z = 10$

atom	site	*x*	*y*	*z*	*B*(Å^2)	f_{occ}
Ir1	2a	0.0	0.0	0.0	3.2(4)	1.0
Ir2	4i	−0.4529(12)	0.0	0.8215(8)	1.03(16)	1.0
Ir3	4i	−0.6046(14)	0.0	0.5920(10)	2.4(2)	1.0
Ba1	2c	0.5	0.5	0.5	1.2(5)	1.0
Ba2	4i	−0.191(2)	0.0	0.7139(12)	0.1(3)	1.0
Ba1	4i	−0.247(2)	0.5	0.8886(15)	0.9(3)	1.0
O1	8j	0.053(2)	0.721(3)	0.7002(13)	2.3(3)	1.0
O2	8j	−0.0093(15)	−0.771(2)	0.1085(11)	1.2(3)	0.923(4)
O3	4i	0.703(4)	0.0	0.303(3)	4.0(6)	1.0
O4	4i	0.217(2)	0.	0.0607(12)	0.6(2)	1.0
O5	2d	0.5	0.0	0.5	1.5(5)	1.0
O6	4f	0.75	0.75	0.5	3.9(5)	1.0

[a] Discrepancy factors: $R_p = 2.40\%$, $R_{wp} = 3.22\%$, $R_{exp} = 1.28\%$, $\chi^2 = 6.34$, $R_{Bragg} = 9.35\%$.

The crystal structure is defined in the *C*2/*m* space group with three kinds of Ba atoms at 2c (*0.5,0.5,0.5*) and 4i (*x,0,z*), three types of Ir atoms at 2a (*0,0,0*) and 4i sites, and six inequivalent oxygen atoms at 8j (*x,y,z*), 4i, 2d (*0.5,0,0.5*), and 4f (*0.75,0.75,0.5*) positions. The occupancy factors of all the oxygen atoms were refined; those of O1, O3, O4, O5, and O6 converged to values slightly higher than unity and then they were fixed to 1.0; for O2 the occupancy factor converged to 0.923(4). This implies a crystallographic formula $BaIrO_{2.938(3)}$, slightly oxygen deficient in agreement with the thermal analysis data for the starting material ("9R" phase).

Table 3 contains the atomic parameters after the refinement, and Table 4 lists the main bond distances and angles; the Rietveld plot is shown in Figure 4. As illustrated in Figure 5a, the crystal structure of the 5H polytype can be described as a stacking of layers of corner sharing (*c*) and face sharing (*h*) IrO_6 octahedra along the sequence *hchcc*. The structure contains chains of double dimer units of $Ir2O_{6/2}-Ir3O_{6/2}$ octahedra sharing faces via O1 and O3 oxygens along the *c*-direction; the two twin dimers are corner connected via O5 atoms. These

(13) Brese, N. E.; O'Keeffe, M. *Acta Crystallogr., Sect. B* **1991**, *47*, 192.
(14) Brown, I. D. *Z. Kristallogr.* **1992**, *199*, 255.
(15) Foo, M. L.; Huang, Q.; Lynn, J. W.; Lee, W.-L.; Klimczuk, T.; Hagemann, I. S.; Ong, N. P.; Cava, R. J. *J. Solid State Chem.* **2006**, *179*, 563.
(16) Jordan, N. A.; Battle, P. D. *J. Mat. Chem.* **2003**, *13*, 2220.

Table 4. Main Interatomic Distances (Å) and Angles (deg) of 5H-$BaIrO_3$ from NPD Data at 295 K

IrO_6octahedral			BaO_{12}cuboctahedra		
Ir1	−O2	2.029(15) × 4	Ba1	−O1	3.010(18) × 4
	−O4	1.898(18) × 2		−O3	2.88(3) × 2
<Ir1−O>		1.985		−O5	2.8717(3) × 2
				−O6	2.8733(2) × 4
Ir2	−O1	2.12(2) × 2	<Ba1−O>		2.920
	−O2	1.963(17) × 2			
	−O3	2.23(3)	Ba2	−O1	2.99(3) × 2
	−O4	2.105(18)		−O1	2.77(3) × 2
<Ir2−O>		2.072		−O2	2.635(16) × 2
				−O3	2.879(3) × 2
Ir3	−O1	2.004(17) × 2		−O4	3.25(3)
	−O3	2.11(5)		−O5	3.051(13)
	−O5	1.997(17)		−O6	3.071(15) × 2
	−O6	1.994(7) × 2	<Ba2−O>		2.916
<Ir3−O>		2.017			
			Ba3	−O1	2.87(2) × 2
<Ir−O>		2.033		−O2	3.197(18) × 2
				−O2	2.97(2) × 2
	−O2	2.78(3) × 2		−O3	2.88(5)
Ir2	−Ir3	2.765(16)		−O4	2.936(5) × 2
				−O4	2.57(3)
			<Ba3−O>		2.915
Ir2−O1−Ir3		84.0(10)	<Ba−O>		2.917
Ir1−O2−Ir2		165.1(8)			
Ir2−O3−Ir3		79.1(17)			
Ir1−O4−Ir2		160.3(9)			
Ir3−O5−Ir3		180.0(15)			
Ir3−O6−Ir3		180.0(6)			

clusters of four octahedra are interleaved with single layers of vertex-sharing $Ir1O_{6/2}$ octahedra via O2 oxygens, to form infinite chains along *c*, as shown in Figure 5b. Adjacent chains are interlinked along the *a* and *b* directions via Ir1−O2−Ir2, Ir1−O4−Ir2, and Ir3−O6−Ir3 vertex-sharing bridges as shown in Figure 5c. This is a unique stacking that, with this repetition length, has never been described before among the hexagonal polytypes of ABO_3 perovskites.

Ir−O distances vary in the range 1.90 Å for Ir1−O4 to 2.23 Å for Ir2−O3. The average value, of 2.03 Å, is consistent with the ionic radii sum for Ir^{4+} (0.625 Å) and O^{2-} (1.40 Å).[17] It is noteworthy that the structure contains three kinds of octahedra with rather distinct average sizes: <Ir−O> are 1.985, 2.072, and 2.017 Å for Ir1, Ir2, and Ir3 octahedra. The two largest octahedra, Ir2 and Ir3, are those forming dimers, where the Ir−O bonds are weakened by the Ir−Ir bonds. Additionally, these Ir cations are linked to O2, for which a slight oxygen deficiency was detected. According to these bond distances, the bond valences for the three types of octahedra are 4.26(8)+, 3.35(8)+, and 4.06(9)+, indicating that Ir1 and Ir2 are under certain compressive and tensile stresses, respectively. Within the Ir_2O_9 dimers, the Ir2−Ir3 bondlengths are 2.77 Å. This distance is conspicuously larger than the separation of 2.72 Å found in Ir metal, which suggests a weaker metal−metal bond between iridium cations across the shared faces of adjacent octahedra within the dimers because of the coulomb repulsive force between them. The Ba−O distances of the three Ba atoms range between 2.57(3) Å for Ba3−O4 and 3.197(18) Å for Ba3−O2. For Ba1 and Ba2 the coordination polyhedra can be considered to be formed by 8 short + 4 long distances, whereas for Ba3 it is constituted of 6 + 6 bonds. The average distances are very similar for the three polyhedra, with <Ba−O> = 2.917 Å.

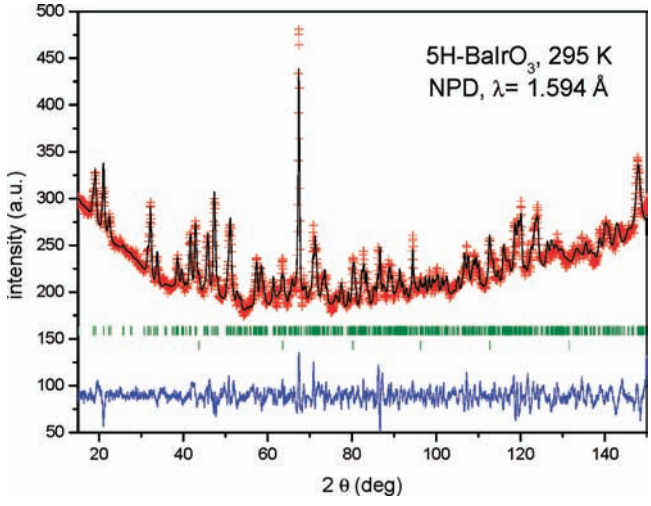

Figure 4. Observed (crosses), calculated (full line), and difference (down) NPD profiles after the structural refinement of the 5H $BaIrO_3$ crystal structure at 295 K. The two series of allowed Bragg reflections (vertical marks) correspond to the main phase and vanadium metal from the sample holder.

6H polytype. This phase was stabilized at pressures of 5 GPa and higher. Figure 6 shows the XRD pattern obtained at 10 GPa, which could be indexed in a monoclinic unit cell with $a = 5.7483(2)$ Å, $b = 9.9390(3)$ Å, $c = 14.3582(5)$ Å, $\beta = 91.319(2)°$. In fact, it consists of a monoclinic distortion of the standard 6H structure, defined in the hexagonal space group $P6_3/mmc$. In this case, the crystal structure was refined in the $C2/c$ space group taking as starting model that of $Ba_3CaIr_2O_9$.[18] The two kinds of Ba atoms were placed at 4*e* (*0,y,1/4*) and 8*f* (*x,y,z*) positions; Ir1 was located at 4*a* (*0,0,0*) and Ir2 at 8*f* sites, and the five independent positions for oxygen atoms, O1 at 4*e*, O2, O3, O4 and O5 at 8*f* positions. Tables 5 and 6 list the main atomic parameters and interatomic distances and angles for this 6H-$BaIrO_3$ polytype. Figure 7a includes a view of the crystal structure of 6H-$BaIrO_3$. It consists of dimers of Ir2 face-sharing octahedra separated by single Ir1 corner sharing octahedra, showing the sequence *hcchcc* along the *c*-axis. It is clear that it contains two distinct metal sites, Ir1 shares only vertices with adjacent octahedra while Ir2 shares both vertices and faces with neighboring octahedra. The $Ir2O_{6/2}$ octahedra within the dimers are considerably more expanded than the $Ir1O_{6/2}$ octahedra, with average Ir−O distances of 2.16 and 1.99 Å, respectively. This is probably a consequence of the metal−metal bond linking the couples of Ir2 atoms in the dimers, with Ir2−Ir2 distances of 2.710(3) Å, which is shorter than in the 5H polytype. As a result of the different octahedral sizes, the bond valences for Ir1 and Ir2 are 4.3(2)+ and 2.8(1)+, respectively. The Ba coordination polyhedra exhibit Ba−O distances between 2.44(3) Å for Ba2−O4 and 3.52(3) Å for Ba1−O4; for Ba1 the distances are distributed as 8 short + 4 long, whereas for Ba2 the bond-length distribution is 6 + 6. Both Ba polyhedra show similar average, <Ba1−O> = 2.90 Å and <Ba2−O> = 2.89 Å.

3C polytype. The 6H polytype was identified at three pressures: 5 GPa, 7.5 and 10 GPa. During the refinement of the crystal structure of the 6H phase obtained at 10 GPa from XRD data, a disagreement observed in certain reflections, at Bragg positions corresponding to the perovskite aristotype, made

(17) Shannon, R. D. *Acta Crystallogr., Sect. A* **1976**, *32*, 751.
(18) Sakamoto, T.; Doi, Y.; Hinatsu, Y. *J. Solid State Chem.* **1976**, *19*, 213.

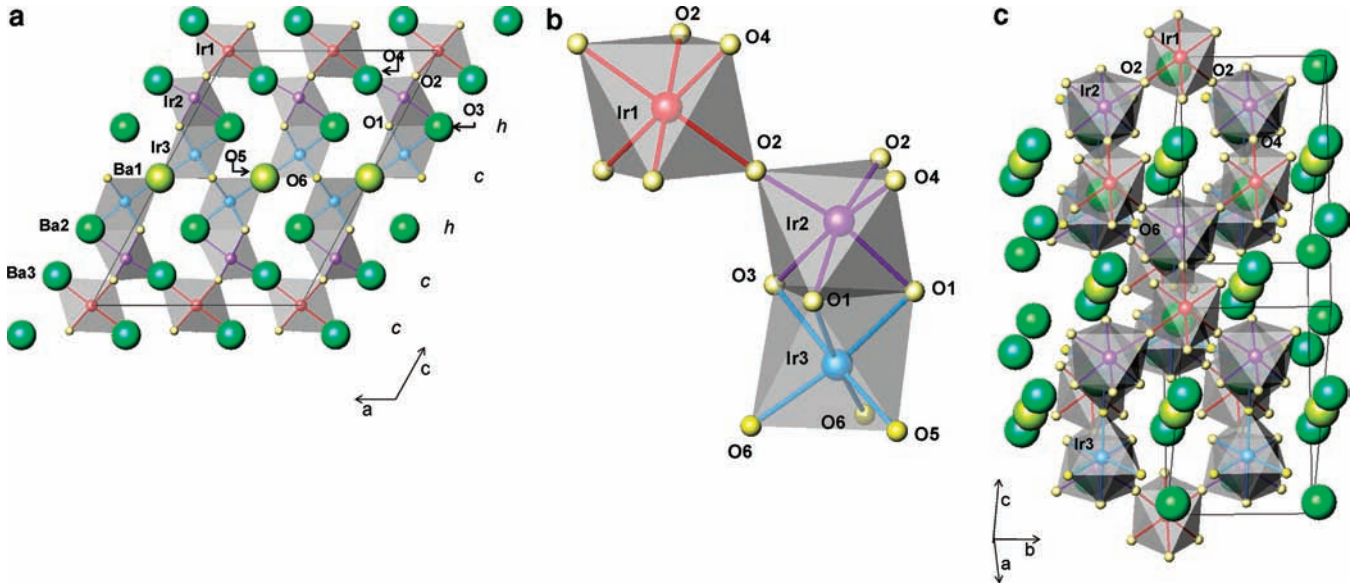

Figure 5. Three views of the crystal structure of the 5H polytype, (a) along [0 1 0], highlighting the stacking of hexagonal (h) and cubic (c) layers corresponding to face-sharing or vertex-sharing IrO_6 octahedra, (b) close up of the dimer formed by $Ir2O_6$ and $Ir3O_6$ face-sharing octahedra, connected to $Ir1O_6$ by vertex sharing via O2 and O4 oxygens (b), approximately along the [1 0 1] direction.

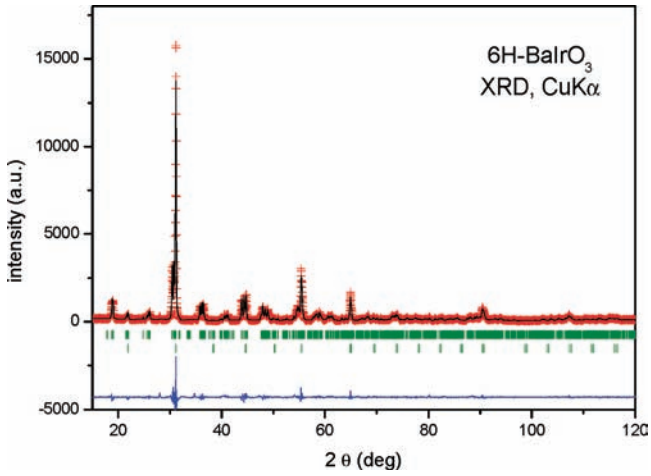

Figure 6. XRD pattern of the 6H-$BaIrO_3$ polytype obtained at 10 GPa, after the Rietveld refinement of its crystal structure, defined in the monoclinic *C*2/*c* space group. The first series of tick marks correspond to the main 6H phase (95%) and the second series to the 3C $BaIrO_3$ structure, identified as a minority phase (5%) at this pressure.

Table 5. Atomic Coordinates and Isotropic Thermal Factors B_{iso} [Å^2] for 6H-$BaIrO_3$ from Powder XRD Data[a] at 295 K; Space Group *C*2/*c*, a = 5.7483(2) Å, b = 9.9390(3) Å, c = 14.3582(5) Å, β = 91.319(2)°, V = 820.12(5) Å^3, Z = 12

atom	site	*x*	*y*	*z*	B_{iso}
Ba1	4e	0.0	−0.0052(6)	0.25	0.3(1)
Ba2	8f	0.0078(6)	0.3349(6)	0.0912(2)	0.25(8)
Ir1	4a	0.00000	0.00000	0.0	0.4(1)
Ir2	8f	0.9936(4)	0.3323(4)	0.8442(1)	0.27(5)
O1	4e	0.0	0.499(4)	0.25	−0.2(3)
O2	8f	0.218(5)	0.239(3)	0.2427(16)	−0.2(3)
O3	8f	0.036(5)	0.846(4)	0.0852(17)	−0.2(3)
O4	8f	0.286(6)	0.087(3)	0.049(2)	−0.2(3)
O5	8f	0.809(6)	0.090(3)	0.103(2)	−0.2(3)

[a] Discrepancy factors: R_p = 9.22%, R_{wp} = 12.2%, R_{exp} = 6.38%, χ^2 = 3.62, $R_{Bragg(6H)}$ = 4.90%, $R_{Bragg(3C)}$ = 2.48%.

it advisible to introduce as a second phase a perovskite model for $BaIrO_3$ defined in the space group $Pm\bar{3}m$ with Ir at 2a (*0,0,0*), Ba at 2b (*0.5,0.5,0.5*) and O at 3c (*0.5,0,0*) sites. The refinement converged with excellent discrepancy factors for both 6H (R_{Bragg} = 4.90%) and 3C (R_{Bragg} = 2.48%) polytypes. From the scale factors, it was possible to estimate the amount of 3C phase as 5%. The volume fraction of 3C phase in the syntheses at 5 GPa and 7.5 GPa was negligible. The unit cell parameter of this ideal perovskite phase is 4.0611(7) Å. This is expected to be the high-pressure phase of $BaIrO_3$, which could not be stabilized pure under our maximum pressure conditions ($P \leq$ 10 GPa) but, at least, it could be identified as a minority phase at 10 GPa. The coexistence of the two polymorphs, 6H and 3C, at 10 GPa is probably due to the fact that during the high-pressure experiment the sample, of ceramic nature, does not experience a purely hydrostatic pressure, but undergoes a certain pressure inhomogeneity, suffering in localized areas an excess pressure (in the contact regions between adjacent microcrystals)

Table 6. Main Interatomic Distances (Å) and Angles (deg) of 6H-$BaIrO_3$ from Powder XRD Data at 295 K

IrO_6octahedra			BaO_{12}cuboctahedra		
Ir1	−O3	1.93(3) × 2	Ba1	−O1	2.8743(3) × 2
	−O4	2.02(3) × 2		−O2	2.78(3) × 2
	−O5	2.01(3) × 2		−O2	2.97(3) × 2
<Ir1−O>		1.99		−O3	2.76(3) × 2
				−O4	3.52(3) × 2
				−O5	2.51(3) × 2
Ir2	−O1	2.19(4)			
	−O2	2.22(3)	<Ba1−O>		2.90
	−O2	2.23(3)			
	−O3	2.10(4)	Ba2	−O1	2.77(3)
	−O4	2.09(3)		−O2	2.65(3)
	−O5	2.11(4)		−O2	2.88(3)
<Ir2−O>		2.16		−O3	3.16(3)
<Ir−O>		2.10		−O3	2.73(3)
Ir2	−Ir2	2.710(3)		−O3	3.03(3)
				−O4	3.04(3)
Ir2−O1−Ir2		76.4(15)		−O4	2.85(3)
Ir2−O2−Ir2		75.1(10)		−O4	2.44(3)
Ir1−O3−Ir2		164.4(15)		−O5	2.77(3)
Ir1−O4−Ir2		151.4(12)		−O5	3.00(3)
Ir1−O5−Ir2		153.6(14)		−O5	3.40(3)
			<Ba2−O>		2.89

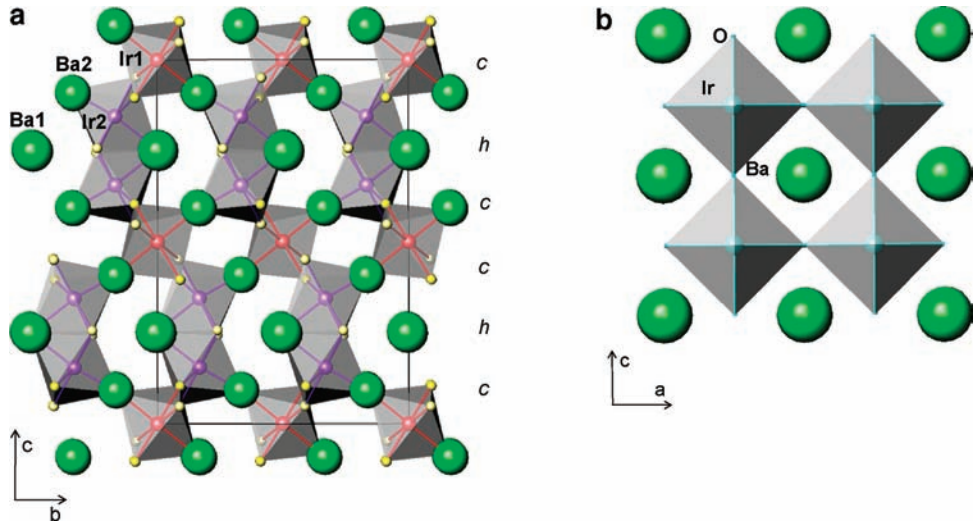

Figure 7. Crystal structures of (a) 6H polytype of $BaIrO_3$, showing the stacking sequence $(hcc)_2$ and (b) 3C polytype or aristotype of $BaIrO_3$, where regular IrO_6 octahedra share corners along the three crystallographic directions.

that can favor the transformation to the higher-pressure polymorph. As shown in Figure 7b, it consists of an arrangement of regular IrO_6 octahedra sharing vertices with an Ir−O−Ir angle of 180° and Ba cations in 12-fold coordination in the center of the cuboctahedral voids. The Ir−O distances are 2.0306(4) Å with a corresponding bond valence for Ir cations of 3.89+, close to the expected value of 4+. Ba atoms are coordinated to 12 atoms at equal distances of 2.8717(5) Å.

Discussion

As a general trend, the A−O bond is more compressible than the B−O bond in ABO_3 perovskites; therefore, the A−O bond length decreases more rapidly with pressure, and so does the tolerance factor ($dt/dP < 0$), leading to the stabilization of the cubic vs hexagonal stacking. This is also consistent with pressure stabilizing preferentially the denser phase since in the 3C perovskite A cations exhibit 12-fold oxygen coordination whereas in the hexagonal polytypes this coordination is reduced to 6 + 6 or lower. The observed crystallographic densities of the "9R", 5H, 6H, and 3C phases of $BaIrO_3$ were 8.84, 9.08, 9.17, and 9.36 g/cm^3, respectively. They progressively increase as expected since these phases have been stabilized at increasing pressures; the 3C perovskite was identified as a minority phase together with the 6H polytype at 10 GPa. This sequence corresponds, therefore, to more dense packings of the BaO_3 layers along the *c*-axis, showing an evolution to structures with more corner-sharing and fewer face sharing octahedra, corresponding to a decreasing value of the tolerance factor under pressure. In fact, the Ba coordination polyhedra become progressively more regular with lower deviations from the average distances.

It is evident that the application of external pressure destabilizes the structures with multiple face-sharing octahedra as the cations are forced closer together. Eventually, the cation repulsion exceeds the metal−metal bonding involved in the octahedral face-sharing. In general, the intermediate polytypes occur only in a narrow transitional interval of the tolerance factor. Because Δt is small, it is possible to find examples where the various polytypes are stabilized successively with increasing pressure. The classical sequence 2H → 9R → 4H → 6H → 3C was described by Longo et al.[19] and Dance et al.[20] The paradigmatic example of $BaRuO_3$ has been intensively investigated. As mentioned in the introduction, it shows a pressure evolution along the sequence 9R-4H-6H-3C.[2] Similar behavior has been described for many oxides, fluorides and chlorides; for instance $CsMnCl_3$ transforms from the ambient pressure 9R structure to the cubic 3C polytype via a 6H structure.

The interval of pressure stability of the 5H polytype of $BaIrO_3$ is probably smaller than 1 GPa. Experiments performed at 3 GPa yielded the pure "9R" polytype, at 4 GPa the 5H phase was stabilized as a pure phase, whereas at 5 GPa the 6H polytype was formed. The stability range of 5H-$BaIrO_3$ is, therefore, very narrow, which explains why it was not described before. There is a reference to the formation of 6H-$BaIrO_3$ at 5 GPa, in agreement with our observation, but no details on this polytype have been published.[21] On the other hand, the synthesis of 5H-$BaIrO_3$ was shown to be perfectly reproducible under the same conditions, as verified when preparing the large sample for the NPD study obtained from 8 HPHT experiments yielding single-phase products with identical XRD patterns.

In order to understand the sequence of transitions observed in $BaIrO_3$, comparison with the $BaRuO_3$ case is enlightening. In this compound the 9R ambient-pressure structure, with a stacking sequence $(chh)_3$, containing 1/3 of cubic vs hexagonal stacking, transforms at 3 GPa into the 4H (*hchc*) polytype, having equal amounts of cubic and hexagonal stackings. Finally, at 5 GPa there is a phase transition to the 6H $(cch)_2$ polytype containing 2/3 of cubic stacking. In spite of the slightly smaller tolerance factor of $BaIrO_3$ ($t = 1.051$) with respect to $BaRuO_3$ ($t = 1.054$), which would normally require a lower external pressure to induce the first phase transition, $BaIrO_3$ does not undergo a structural transformation up to 4 GPa where pressure stabilizes a 4H-6H hybrid polytype 5H (*hchcc*) having a higher proportion of cubic stacking (3/5) than the 4H structure. The reason for this different behavior is certainly related to a higher stability of "9R"-$BaIrO_3$ with respect to 9R-$BaRuO_3$. Let us recall that the $BaRuO_3$ crystal structure is defined in the

(19) Longo, J. M.; Kafalas, J. A. *Mater. Res. Bull.* **1968**, *3*, 687.
(20) Dance, J. M.; Tressaud, A. *Mater. Res. Bull.* **1979**, *14*, 37.
(21) Zhao, J. G.; Yang, L. X.; Yu, Y.; Li, F. Y.; Yu, R. C.; Jin, C. Q. *J. Solid State Chem.* **2009**, *182*, 327.

rhombohedral space group $R\bar{3}m$ whereas $BaIrO_3$ exhibits a monoclinic distortion with the same basic stacking sequence. The main difference between both crystal structures is that whereas the Ru−Ru distance in $BaRuO_3$ is relatively short, 2.55 Å,[15] the Ir−Ir distance in "9R"-$BaIrO_3$ is considerably longer, 2.622(3) Å for Ir1−Ir2 and 2.644(3) Å for Ir3−Ir4. These longer distances are associated with the larger spatial extension of the Ir 5d orbitals, accounting for a longer equilibrium distance for the balance between the coulomb repulsion and the metal−metal bonding, even though the ionic sizes of Ir^{4+} (0.625 Å) and Ru^{4+} (0.620 Å) are very similar[17] in octahedral coordination. Also, a greater number of d electrons on the Ir^{4+} ions than the Ru^{4+} ions leads to weaker, longer bonds to oxygen, and to estimated bond valences for Ir significantly smaller than 4+. The longer Ir−Ir distances across the face-sharing octahedra make this structure considerably more stable toward an external applied pressure, in a range $P < 4$ GPa. At 4 GPa, stabilization of a polymorph with a greater proportion of cubic stacking than that of the 4H phase is required, leading to the formation of the 5H polymorph where the size of the three kinds of $IrO_{6/2}$ octahedra are more similar and the charge distribution corresponds more precisely to the expected 4+ value. This intermediate phase has the particularity of showing a considerably longer Ir−Ir distance within the dimers of face-sharing octahedra, 2.76 Å, implying a weaker metal−metal bonding and a stronger Ir−O bonding. Finally, the subsequent application of increasing external pressure leads to the collapse of this phase, giving rise to the 6H polymorph with smaller Ir−Ir bond lengths of 2.71 Å. It is a delicate balance between the external pressure and the Ir−Ir repulsion across the face-sharing octahedra and the trend to decrease the hexagonal vs cubic packing ratio that makes possible the formation of this unreported polymorph in an extremely narrow range of pressures.

Another clue for understanding the significant stability of the ambient pressure "9R"-$BaIrO_3$ phase can be related to the particular stability of $SrIrO_3$, which despite a tolerance factor below unity ($t = 0.97$) prefers to adopt the hexagonal 6H polytype instead of the 3C perovskite structure at ambient pressure, whereas most of the remaining $SrBO_3$ compounds (B = Ti, Zr, Hf, Mo, Cr, Ru, Fe, Sn, Pb) form 3C perovskites. It would appear that the hexagonal polytype is stabilized by the cubic-field outer electron configuration $t_{2g}^5e_g^0$ for low-spin Ir(IV). In the trigonal field of the hexagonal polytype the t_{2g}^5 orbitals become $e_{g\sigma}^0e_{g\pi}^4a_{1g}^1$, which allows for metal−metal bonding along the c-axis via the half-filled a_{1g} orbitals. Simultaneously, the 90° Ir−O−Ir $\pi-\sigma$-bond interactions are strengthened. The reinforcement of the Ir−O bonds as well as the formation of stable Ir−Ir bonds seem to stabilize the hexagonal polytypes for $AIrO_3$ compounds, thus accounting for the pressure stability of the "9R"-$BaIrO_3$ phase containing a large ratio of h vs c packing.

It is noteworthy that the three polytypes "9R", 5H and 6H exhibit a monoclinic symmetry. Whereas for the "9R" and 6H structures the monoclinic β angles are close to 90°, implying that the chains of face-sharing octahedra are almost perpendicular to the *ab* plane, the 5H polytype presents a β angle of 119.23°, involving an arrangement where the chains of octahedra are extremely shifted and leaned with respect to the *ab* plane. This particular arrangement involves a reduced tilting of the IrO_6 octahedra as far as corner sharing is concerned, giving 180° angles for Ir3−O5−Ir3 and Ir3−O6−Ir3 (Table 4), which promotes a full overlap between Ir-$e_{g\sigma}^0$ and O-2p orbitals. The formation of these strong σ bonds between Ir atoms of adjacent chains could be the driving force for exceptional monoclinic distortion. The mentioned overlap suggests improved transport properties for the 5H polytype with respect the ambient-pressure phase, containing more bent tilting angles interconnecting the chains of octahedra, of 155.4(11)° for Ir1−O1−Ir3 and 164.2(10)° for Ir1−O2−Ir3 (Table 2).

The 5H-$BaIrO_3$ phase is the first example of a 5H polytype of a stoichiometric, single-valent perovskite showing *hchcc* stacking. Other phases with a so-called 5H structure have been described in different systems, but they correspond to defective perovskites with different octahedral stackings than that observed in 5H-$BaIrO_3$. Compounds of stoichiometry $BaIr_{1-x}Co_xO_{3-\delta}$ ($x = 0.5, 0.7, 0.8$)[22] have been reported to adopt 12R, 10H, and 5H perovskite structures, respectively, where the distribution of Co and Ir cations over corner-sharing and face-sharing sites has been determined and the Co/Ir−O bond lengths have been used to assign the cation oxidation states as Ir^{5+} and Co^{3+}/Co^{4+}. The 5H polytype of $BaIr_{0.2}Co_{0.8}O_{2.84}$ is characterized by *hhccc* stacking, where $(Co/Ir)_3O_{12}$ trimers of face-sharing octahedra are separated by two layers of corner-sharing octahedra exclusively occupied by Co. Moreover, some oxygen deficiency is found between the two Co layers of octahedra containing a BaO_2 layer instead of a BaO_3 layer, as observed in 12H $BaCoO_{2.6}$.[23] The reduction of this layer results in the replacement of two corner-sharing octahedra by two unconnected tetrahedra. Something similar is observed in the defective perovskite $BaMn_{0.2}Co_{0.8}O_{2.80}$,[24] the structure of which can be described as a *cc′chh* 5H hexagonal polytype with ordered oxygen vacancies where the cubic c' layer corresponds to a composition of $[BaO_2]$ as opposed to $[BaO_3]$. The resulting layer structure consists of $[MnCo_2O_{12}]$ blocks of three face-sharing octahedra linked by corners to two unconnected $[CoO_4]$ tetrahedra. This stacking sequence is in contrast with that observed in the present work for 5H-$BaIrO_3$, characterized by the *hchcc* sequence, in the sense that (i) no oxygen deficiency has been detected in 5H-$BaIrO_3$ by neutron diffraction so the octahedral connection is complete along the c-axis and (ii) although both sequences involve the same proportion of h and c stackings, *hhccc* present a lower number of changes from hexagonal to cubic and thus it would, in principle, exhibit a higher thermodynamic stability.[1]

A polytypoid 5H with the stacking sequence *chhcc* has also been described for a well-known family of defective perovskites of general stoichiometry $A_5B_4O_{15}$ (for instance $Ba_5Nb_4O_{15}$ or $Ba_5Ta_4O_{15}$), defined in the space group $P\bar{3}m1$ and characterized by the presence of a fully ordered distribution of cations and vacancies at the B sublattice.[25] In this structure, which contains chains of three face-sharing octahedra, the vacancies are located in the central octahedron, leading to a maximum separation of the highly charged (e.g., Nb^{5+} or Ta^{5+}) cations.

Finally, very few compounds have been found to crystallize in the rare 15R modification. A paradigmatic example is $BaIr_{0.3}Fe_{0.7}O_{2.95}$, defined in the space group $R\bar{3}m$, with $a \approx 5.73$ Å, $c \approx 35.55$ Å. There are two possible stacking sequences that yield such a cell; these correspond to the $(hhhhc)_3$, which has been reported for the system $BaMnO_{3-\delta}$,[26] and the $(cchch)_3$

(22) Vente, J. F.; Battle, P. D. *J. Solid State Chem.* **2000**, *152*, 361.
(23) Jacobson, A. J.; Hutchison, J. L. *J. Solid State Chem.* **1980**, *35*, 334.
(24) Miranda, L.; Feteira, A.; Sinclair, D. C.; García-Hernández, M.; Boulahya, K.; Hernando, M.; Varela, A.; González-Calbet, J. M.; Parras, M. *Chem. Mater.* **2008**, *20*, 2818.
(25) De Paoli, J. M.; Alonso, J. A.; Carbonio, R. E. *J. Phys. Chem. Solids* **2006**, *67*, 1558.
(26) Negas, T.; Roth, R. S. *J. Solid State Chem.* **1979**, *3*, 323.

observed for $SrFe_{0.085}Mn_{0.915}O_{2.979}$[27] and $BaIr_{0.3}Fe_{0.7}O_{2.949(7)}$.[28] This stacking is similar to that of the 5H polytype described in the present work, but it acquires a triple periodicity. The 15R structure comprises dimers of face-sharing octahedra as well as octahedra that share only vertices with their neighbors. For $BaIr_{0.3}Fe_{0.7}O_{2.949(7)}$,[28] the delicate balance between the stabilities of the 6H and 15R polytypes was highlighted by the presence of a small amount of the 6H phase together with the main 15R phase. This observation is in full agreement with the present findings for the 5H-$BaIrO_3$ polytype, which showed a precarious range of stability, giving way to the 6H phase upon a small increment of the external pressure.

Conclusions

In summary, the sequence of pressure-induced transitions of $BaIrO_3$ has been studied in the pressure range up to 10 GPa. Four phases have been identified, the so-called "9R", 5H, 6H, and 3C structures. The 5H-$BaIrO_3$ phase is the first example of a 5H polytype of a stoichiometric, single-valent perovskite showing *hchcc* stacking. Other phases with a so-called 5H structure have been described in different systems, but they correspond to defective perovskites with different octahedral stackings than that observed in 5H-$BaIrO_3$. The significant stability found for the "9R" polytype, identified up to 3 GPa, accounts for the formation of this new 5H polytype at 4 GPa: the *hchcc* sequence has a higher ratio of cubic stacking than the commonly found 4H phase with the *hchc* sequence. The pressure stability of the "9R" phase is related to a strong metal−metal bonding in spite of the long Ir−Ir distances observed within the trimers of face-sharing octahedra, of 2.67 Å, given the spatial extension of the 5d orbitals involved in the metal−metal bonding. The Coulombic repulsion between the Ir^{4+} ions is responsible for the displacement of Ir3 and Ir1 away from Ir2 and Ir4 at the center of the trimers, but the Ir−Ir bonding reduces the magnitude of that displacement and allows pressure to decrease this distance before a new polytype is stabilized. The intermediate 5H phase relieves the Coulombic repulsion by giving an even larger Ir−Ir distance within the dimers of face-sharing octahedra, of 2.77 Å, implying a weaker metal−metal bonding and a stronger Ir−O bonding; the stability pressure range of this phase is small (less than 1 GPa), and the subsequent application of increasing external pressure leads to the collapse of this phase to give the 6H polytype with a smaller Ir−Ir bond length of 2.71 Å. A delicate balance between the increased Ir−Ir bonding with the external pressure and the Ir−Ir repulsion across the face-sharing octahedra, as well as the trend to decrease the hexagonal vs cubic packing ratio, makes possible the formation of this unreported 5H polymorph in an extremely narrow range of pressures. Finally, the cubic 3C perovskites were identified as a minority phase at 10 GPa, but it was not possible to isolate it as a pure phase in the available pressure range.

Acknowledgment. We are grateful to ILL for making the beamtime available. J.S.Z. and J.B.G. thank the NSF for financial support. J.A.A. acknowledges the financial support of the Spanish "Ministerio de Ciencia e Innovación" to the project MAT2007-60536 and during his sabbatical.

JA901829E

(27) Cussen, E. J.; Sloan, J.; Vente, J. P.; Battle, P. D.; Gibb, T. C. *Inorg. Chem.* **1998**, *37*, 6071.
(28) Jordan, N. A.; Battle, P. D.; Sloan, J.; Manuel, P.; Kilcoyne, S. *J. Mat. Chem.* **2003**, *13*, 2617.